Pressure-Based Long-Range Correction for Lennard-Jones Interactions in Molecular Dynamics Simulations: Application to Alkanes and Interfaces

Patrick Lagüe and Richard W. Pastor

Laboratory of Biophysics, Center for Biologics Evaluation and Research, FDA, 1401 Rockville Pike, Rockville, Maryland 20852-1448

Bernard R. Brooks*

Laboratory of Structural Biology, Division of Computer Research & Technology, National Institutes of Health, Bethesda, Maryland 20892

Received: April 17, 2003; In Final Form: October 3, 2003

A straightforward method that accounts for the long-range Lennard-Jones (LJ) terms in constant pressure molecular dynamics simulations is presented. This long-range correction (LRC) consists of an additional applied pressure tensor which is periodically calculated from the difference of instantaneous pressures at the selected cutoff and a very long cutoff. It provides results that are nearly independent of the LJ cutoff distance at negligible additional calculation costs, and is particularly suited for anisotropic systems such as liquid/liquid interfaces or heterogeneous macromolecules where approximations based on spherically symmetric radial distribution functions are expected to fail. The utility of the method is demonstrated for a series of alkanes and water, and for interfaces including a lipid bilayer. The LRC increases densities and decreases isothermal compressibilities, with the changes larger for alkanes than for water (where the long-range interactions are dominated by electrostatic interactions). While implementation of the LRC will not necessarily improve agreement with a particular experiment, it will provide a baseline for improvements in a parameter set that are consistent with the long-range Lennard-Jones interactions.

Introduction

The most time-consuming part of molecular dynamics (MD) simulations of fluids and macromolecules is the computation of the electrostatic and Lennard-Jones (LJ) interaction energies. In early simulations these long-range interactions were often set to zero at relatively short separation distances. To reduce computer time, numerous approximation methods have been employed to limit the cost of long-range interactions while trying to mitigate the artifacts due to the neglect of interactions beyond a cutoff distance.[1,2] Upon the examination of artifacts related to truncation of electrostatic terms,[3−5] the technique of Ewald summation, commonly used in simulation of pure liquids, was adopted for use and is now standard in most simulations of polar or charged macromolecular systems. Formally, Ewald summation is exact, although numerical errors associated with the representation of the reciprocal space and the choice of boundary conditions need to be considered. In contrast, there is presently no computationally efficient equivalent approach for LJ terms in macromolecular systems. It is possible to evaluate the LJ potential with an Ewald summation approach, but this is only practical when the number of different atom types is very small.[5,6] In the typical case involving macromolecules, there are dozens of atom types with different LJ parameters, resulting in the need to employ another method to limit computational costs. Nevertheless, the need to consider long-range LJ energy terms is clear: they are always attractive and thereby do not cancel.

There have been two basic approaches for reducing errors arising from neglect of long-range LJ terms in periodic systems. The more recent involves extending the cutoff, r_c, to 14−30 Å.[7,8] This is computationally inefficient when combined with treating the electrostatic interactions with Ewald summation (where $r_c \approx 10-12$ Å provides an effective balance between the real and reciprocal space computations), and may require reparametrization of already established force fields. Another approach involves evaluating corrections to thermodynamic quantities such as energy, pressure, and chemical potential from their statistical mechanical expressions under the assumption that the radial distribution function $g(r) \approx 1$ for $r > r_c$.[1] The long-range correction (LRC) is then a simple function of r_c and the average density. This LRC has been used in simulations of neat liquids, and LJ parameters in recent versions of the CHARMM force field have been optimized against calculated densities from such simulations.[9] This approximation will be expected to break down for systems with interfaces, where the composition and density depend on direction.

This study presents a LRC appropriate for constant pressure ensembles that avoids the complications and inefficiencies described above. In essence, instantaneous pressures are calculated at relatively short (10−12 Å) and very long (30 Å) cutoffs, and the difference ΔP is determined. The simulation is carried out at the short cutoff with the additional pressure ΔP, and the value of ΔP is updated as necessary. For anisotropic systems ΔP is a tensor, and the individual components are applied separately. For this method to be effective, it must be demonstrated that the ΔP tensor exhibits no significant drift between updates.

A variety of systems were simulated to test the validity and utility of this simple technique: bulk water, a range of alkanes from heptane to eicosane, water/vacuum, heptane/vacuum,

10.1021/jp030458y
Published on Web 12/04/2003

heptane/water interfaces, and a dipalmitoylphosphatidylcholine (DPPC) lipid bilayer. As appropriate, densities, diffusion constants, isothermal compressibilities, surface tensions, and NMR ^{13}C T_1 relaxation times were evaluated and compared with experiment.

Methods

Simulation Details. Simulations were performed with the program CHARMM[10] using the CHARMM27 all-atom potential energy parameter set[11] with modified TIP3P waters.[12,13] Electrostatic interactions were calculated via the particle mesh Ewald (PME) method,[3] with $\kappa = 0.34$ Å^{-1} and a fast-Fourier grid density
≈ 1 Å^{-1}. Cutoffs for the real space portion of the PME calculation and for the truncation of the LJ interactions were 10 Å, unless otherwise specified, with the latter smoothed via a switching function over the range of 8−10 Å. SHAKE[14] was used to constrain all covalent bonds involving hydrogen atoms. All simulations employed the leapfrog Verlet algorithm and three-dimensional orthorhombic periodic boundary conditions. To ensure that our observations are not affected by time step artifacts, we have adapted the relatively conservative time step of 1 fs. Unless otherwise noted, coordinates were saved every 0.1 ps. Nonbond lists were updated heuristically. The thermostat coupling constant was 20 000 kcal ps^2; the piston mass equaled 2500 amu for the DPPC bilayer and 1000 amu for other (smaller) systems. These values avoid artifacts such as oscillations of volume. The following ensembles were used: NPT (for bulk water and alkanes); NVT (bulk heptane and pentadecane, water/vacuum, and heptane/vacuum); NPAT (heptane/water and DPPC bilayer), where N, P, V, A, and T denote particle number, pressure, volume, surface area, and temperature, respectively.

Definitions and Implementation. As appropriate, the value of the cutoff used in calculation of the LJ interactions is subscripted when denoting the instantaneous pressure. Hence, the instantaneous pressure difference is defined as $\Delta P(t) \equiv P_{r_c}(t_0) - P_{r_l}(t_0)$, where r_c and r_l are the short and long cutoffs, respectively, and t_0 is the time of the most recent application of the LRC. To simulate at a target pressure P_0, a trajectory would be propagated with r_c and an applied pressure equal to $P_0 + \Delta P$. Because $P_0 = 1$ atm and $\Delta P \approx 200$ atm for the cases studied here, the applied pressure was simply set to ΔP. Unless specified otherwise, ΔP was updated every 10 ps (10 000 steps). This update period was selected for its computational efficiency, and because it is short with respect to the time scale of significant large-scale reorganization such as bilayer bending, macromolecular rotation, or surface undulation. The notation *ensemble/LRC* (e.g., NPT/LRC) will signify that the long-range correction was applied.

There are two energy terms associated with this LRC. The first is a constant offset between updates, and the second arises from the time integral of ΔP times the rate of change of the volume:

$$\Delta E(t) \equiv (E_{r_c}(t_0) - E_{r_l}(t_0)) + \int_{t_0}^{t} \Delta P \frac{\partial V}{\partial t} \, dt \qquad (1)$$

These two energy terms are both neglected in our current implementation since none of the simulation results presented here depend on them, nor do they enter the propagation equations. For studies where the total system energy is explicitly required (e.g., heats of vaporization), the first term must be included. The second term is only significant when there are large volume changes between updates (usually observed only during heating and equilibration), and it can be ignored.

Even though the value of ΔP was updated every 10 ps for the simulations presented here, alternative update protocols are possible. For example, once the system has reached equilibrium and a sufficient number of values of ΔP have been accumulated, the average ΔP_{ave} and standard deviation $\sigma_{\Delta P}$ could be determined. In principle ΔP_{ave} could be applied as the LRC for the remainder of the simulation, thereby conserving the Hamiltonian. To account for the possibility of dramatic system changes as might occur in the simulation of complex systems, the instantaneous values of ΔP would still be monitored and compared with ΔP_{ave}. If the difference is larger than $4\sigma_{\Delta P}$ in two subsequent comparisons, a new value ΔP_{ave} might be imposed. Perturbations to the Hamiltonian would be infrequent for such a heuristic update procedure.

Initial Conditions. This subsection outlines the assembly and equilibration of each system. Total simulation times varied, and are noted in the tables and figure captions.

The bulk water system consisting of 1000 water molecules was assembled from eight water boxes of 125 water molecules preequilibrated by Monte Carlo simulations. The energy of the system was minimized by alternatively applying 200 steps of both steepest descent (SD) and adopted basis Newton Ralphson (ABNR) methods twice, followed by another 200 steps of SD. Finally, the velocities were initialized at 193.15 K, and the simulation was run for 50 ps with the temperature of the system gradually increased by 10 K every 1 ps, up to 293.15 K.

Each bulk alkane system is composed of 64 molecules. Heptane, hexadecane, and eicosane were assembled from coordinates from previous simulations.[15] The others, dodecane, tridecane, tetradecane, pentadecane, heptadecane, octadecane, and nonadecane, were built by removing a methylene group for each molecule in the coordinate file of the corresponding longer alkane. For each system, the energy was minimized with 50 steps of ABNR, the velocities were initialized at 100 K below the target temperature, and the temperature was then increased by 10 K every 1 ps until the target temperature was reached, and 15 ps of equilibration was carried out. Coordinates were saved every 0.025 ps when reorientational correlation functions were evaluated.

The heptane/water system was constructed by deforming a cubic box of 216 waters preequilibrated by MC simulations into a rectangular prism with area of the previously simulated heptane system (25.17×25.17 Å^2) and height 10.582 Å. The energy was minimized by applying two cycles of 200 steps SD and ABNR, and 200 additional steps of SD. Velocities were initialized at 250.15 K, and the systems were simulated for 5 ps at NVT, with the temperature gradually increased by 10 K every 0.5 ps, up to 312.15 K. This box was added to the top and bottom of the heptane box, and the whole system energy was minimized as described above. Velocities were assigned at 198.15 K, and the simulation was run for 50 ps, with the temperature increased by 5 K every 1 ps, up to 298.15 K.

Water/vacuum and heptane/vacuum were generated from their respective equilibrated bulk systems by expanding the simulation cell along the *z*-axis to yield a vacuum space equal in volume to the original cell. Then, the velocities were initialized at 198.15 K and equilibrated for 50 ps with the temperature increased by 5 K every 1 ps, up to 298.15 K.

The DPPC bilayer consisted of 72 lipids (36 in each leaflet), and 2151 water molecules. The initial configuration was constructed from preequilibrated and prehydrated lipids as described previously,[16−18] with a cross-sectional area of 64 Å^2 per lipid.[19] Velocities were initialized at 223.15 K, and the simulation was run for 50 ps with the temperature increased by

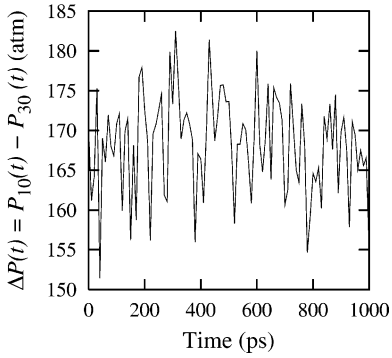

Figure 1. Instantaneous pressure correction for an NPT trajectory of heptane at 312.15 K.

10 K every 1 ps, up to 323.15 K. After 1 ns of equilibration, 10 ns production runs at NPAT and NPAT/LRC were carried out.

Results

Preliminary Testing. To determine the general characteristics of the method, a 1 ns simulation of bulk heptane was carried with a cutoff $r_c = 10$ Å. The internal pressures associated with the LJ energy were calculated at the cutoff used to propagate the trajectory *and* with a 30 Å cutoff. While the instantaneous pressures ranged over a 1000 atm range, the pressure *difference* $\Delta P(t) = P_{10}(t) - P_{30}(t)$ was significantly less variable (Figure 1), with the average of 168 atm and root-mean-square fluctuation of 6 atm. This result implies that the forces associated with the two cutoffs are highly correlated. Consequently, a trajectory carried out with $r_c = 10$ Å and an applied pressure of approximately 170 atm would be expected to yield results similar to one carried out at $r_c = 30$ Å and an applied pressure of 1 atm. The autocorrelation function $\langle \delta\Delta P(0)\ \delta\Delta P(t)\rangle$ is mostly decayed to zero by 10 ps, indicating that the fluctuations in ΔP are mainly due to rapid motion rather than to long-term drift. This supports the argument that 10 ps is a reasonable update frequency for ΔP, at least during equilibration. Heuristic updates following equilibration were discussed in the previous section.

Figure 2 plots the dependence of density and ΔP on cutoff for water, heptane, and pentadecane. Increasing r_c from 10 to 30 Å reduces ΔP from approximately 200 atm to 0 (by definition) and increases density ρ for all three systems. There is essentially no density change at cutoffs larger than or equal to 30 Å, indicating that this value is suitable for r_l.

Bulk Systems. On the basis of the preliminary results described above, trajectories of water and assorted bulk alkanes were carried out with $r_c = 10$ Å, $r_l = 30$ Å, and ΔP updated every 10 ps. Table 1 lists the average densities ρ and isothermal compressibilities β_T for the three systems already discussed, where[1]

$$\beta_T = \frac{1}{V}\left(\frac{-\partial V}{\partial P}\right)_T = \frac{\langle \delta V^2\rangle}{V k_B T} \qquad (2)$$

and $\langle dV^2\rangle$ is the volume fluctuation, k_B is Boltzmann's constant, and T is temperature. The effect of the LRC is relatively small for water (0.7% increase in ρ and a 8% decrease in β_T) but is substantial for the alkanes: an average 3% increase in ρ and 30% decrease in β_T. The preceding density increases can also be estimated by rewriting eq 2 as $\beta_T \Delta P \approx -\Delta V/V$ and substituting $\Delta P = 200$ atm and the values of β_T listed in Table 1. Because the density of modified TIP3P water is approximately

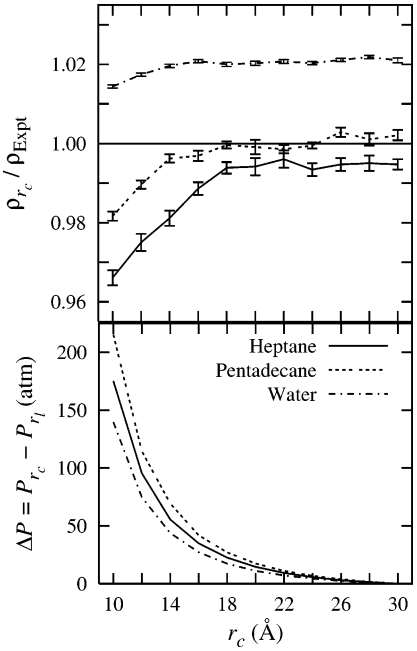

Figure 2. Top: densities relative to the experiment vs cutoff for heptane (solid lines), pentadecane (dashed), and water (dot−dashed) at 293.15 K. Bottom: pressure difference relative to $r_l = 30$ Å for different cutoffs for the preceding systems. Trajectories ranged from 325 ps to 1 ns.

TABLE 1: Densities and Isothermal Compressibilities for Water (at 293.15 K and Trajectory Length 1 ns), Heptane (312.15 K, 1 ns), and Pentadecane (312.15 K, 1.5 ns) from Simulations with the LJ Interactions Cutoff $r_c = 10$ Å (NPT) and with the Long-Range Correction Described in the Text (NPT/LRC)[a]

	ρ (g/cm^3)			β_T (10^{-10} m^2 N^{-1})		
system	water	heptane	penta-decane	water	heptane	penta-decane
NPT	1.0122	0.6354	0.7387	5.2	27.7	12.6
	(0.0003)	(0.0097)	0.0050	(0.1)	(2.7)	(0.7)
NPT/LRC	1.0193	0.6612	0.7539	4.8	16.4	9.5
	(0.0001)	0.0107	0.0140	(0.3)	(0.5)	(0.4)
expt	0.9982	0.6677	0.7552	4.58	15.8	9.2

[a] Standard errors in parentheses.

1% above experiment with $r_c = 10$ Å, applying the LRC increases disagreement with experiment. In contrast, the densities of the alkanes are lower than experiment (4% and 2% for heptane and pentadecane, respectively). In this case, application of the LRC leads to almost quantitative agreement with experiment.

Figure 3 compares the molar volumes for dodecane to eicosane, each at 10 K above its melting temperature, for simulations at NPT, NPT/LRC, and experiment. As for heptane and pentadecane at 312.15 K, application of the long-range correction leads to almost quantitative agreement with experiment (an average error of 0.5% versus 2.1% for NPT). The preceding data yield volumes of methylene and methyl groups from a linear fit of total volume vs carbon number under the assumption $V_{total} = (n-2)V_{CH_2} + 2V_{CH_3}$.[20] As shown in Table 2, agreement with experiment is significantly improved by application of the LRC. Nevertheless, V_{CH_2} is still overestimated by 2% and V_{CH_3} is underestimated by 6%, implying that the good agreement for molar volumes partly results from a cancellation of errors.

Turning to dynamic properties, translational diffusion constants D_t were obtained from weighted linear least-squares fits

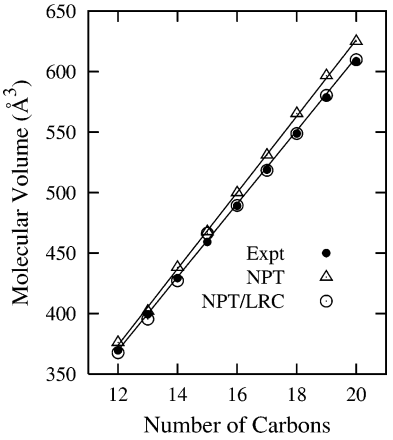

Figure 3. Molecular volumes for selected alkanes, 10 degrees above their respective melting points, from 600 ps simulations at NPT (open circles), NPT/LRC (filled circles), and experiment (open squares); experimental values from ref 20, Table 7-6. The standard errors are smaller than the points' size. Solid lines are results from linear regression.

TABLE 2: Volumes for Methylene and Methyl Groups (V_{CH_2} and V_{CH_3}, respectively) Evaluated from Simulations with (NPT/LRC) and without (NPT) the Long-Range Correction[a]

system	V_{CH_2} (Å^3)	V_{CH_3} (Å^3)
NPT	31.5 (0.1)	29.3 (0.6)
NPT/LRC	30.3 (0.1)	33.4 (0.4)
expt	29.86	35.53

[a] Standard errors in parentheses. Experimental values from ref 20.

TABLE 3: Translational Diffusion Constants for Water and Three Alkanes Evaluated from 1 ns Simulations with (NPT/LRC) and without (NPT) the LRC[a]

	D_t (10^{-5} cm^2 s^{-1})			
system	water (293.15 K)	C7 (312.15 K)	C12 (298.15 K)	C14 (298.15 K)
NPT	4.985 (0.006)	4.061 (0.018)	0.582 (0.002)	0.402 (0.002)
NPT/LRC	4.743 (0.057)	3.268 (0.021)	0.521 (0.002)	0.293 (0.003)
expt	2.02	4.1	0.814	0.520

[a] Standard errors in parentheses. Experimental values are from ref 22 for water, dodecane (C12), and tetradecane (C14) and from ref 23 for heptane (C7).

of the mean squared displacement vs time over the interval 1.0−400 ps, with weights determined from averages over 10 subgroups of molecules.[21] As reported in Table 3 for water and three alkanes, the LRC systematically decreases D_t. This leads to better agreement for water (though the result still substantially overestimates experiment) and worse agreement with experiment for the alkanes. NMR ^{13}C T_1 relaxation times were evaluated from the reorientational correlation functions $\langle P_2(\hat{\mu}(0)\hat{\mu}(t))\rangle$ of CH vectors $\hat{\mu}$ using the standard formula for dipolar relaxation.[24] Assuming motional narrowing, an effective CH bond length of 1.117 Å,[25] and inserting appropriate constants leads to

$$\frac{1}{NT_1} = (1.855 \times 10^{10}\ \mathrm{s}^{-2})\tau \qquad (3)$$

where $\tau = \int_0^\infty \langle P_2(\hat{\mu}(0)\hat{\mu}(t))\rangle\ \mathrm{d}t$ is the rotational correlation time, and N is the number of protons bonded to the carbon of interest. Figure 4 compares the results of simulations carried out at NPT, NPT/LRC, NVT at the experimental density, and experiment. For both heptane and pentadecane, T_1's calculated from NPT/LRC and NVT simulations are almost identical and

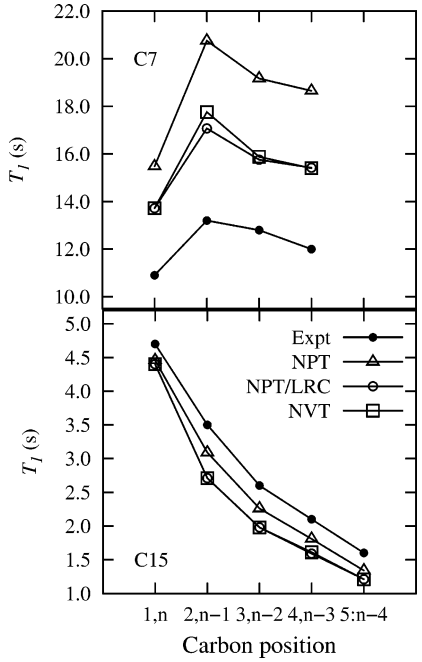

Figure 4. ^{13}C T_1 relaxation times of different carbon positions for heptane (top) and pentadecane (bottom), for NPT (open triangles), NPT/LRC (open circles), NVT (open squares), and experiment (filled circles); experimental values from ref 26. Standard errors are smaller than the points' size. Equilibrium properties for these same sytems are listed in Table 1.

are lower than those obtained from the NPT simulations. These results are consistent with those obtained so far for alkanes, where application of the LRC leads to increased density and decreased translational diffusion constants and, by inference, increased viscosity. Increased viscosity leads to longer rotational tumbling times, larger τ, and, from eq 3, lower T_1's. For heptane, T_1's calculated at NPT are substantially higher than experiment, and therefore applying the LRC increases agreement with experiment. Conversely, T_1's calculated at NPT for pentadecane underestimate experiment, so applying the LRC decreases agreement.

Interfaces. The interfacial or surface tension γ is calculated as

$$2\gamma = \left\langle L_z\left(P_{zz} - \frac{1}{2}P_{xx} - \frac{1}{2}P_{yy}\right)\right\rangle \qquad (4)$$

where L_z is the length of the simulation cell normal to the interface, P_{zz} is the normal component of the pressure tensor, and P_{xx} and P_{yy} are its tangential components.[27] The factor of 2 arises because there are two interfaces in the simulation. The following term approximates the contribution to γ arising from long-range LJ terms:

$$\Delta\gamma = \frac{1}{2}\left\langle L_z\left(\Delta P_{zz} - \frac{1}{2}\Delta P_{xx} - \frac{1}{2}\Delta P_{yy}\right)\right\rangle \qquad (5)$$

where ΔP_{ii} has the same meaning as ΔP (correction terms involving ΔL are very small and can be ignored). This correction is appropriate even when the LRC is not applied, as when calculating the surface tension of a liquid/vacuum interface from a simulation at constant volume, as well as simulations carried out in the NPAT and NPγT ensembles (where the LRC is applied normal to the interface and in all directions, respectively).

It is instructive to begin with liquid/vacuum interfaces, where no LRC is applied. Table 4 compares the surface tensions of

TABLE 4: Surface or Interfacial Tensions (in dyn/cm) at 298.15 K Evaluated from Simulations with $r_c = 10$ Å, $r_c = 25$ Å (Water/Vacuum and Heptane/Vacuum), or LRC (Heptane/Water and DPPC Bilayer)

system	$r_c = 10$ Å	$r_c = 25$ Å	$r_c = 10$ Å/ LRC	$\Delta\gamma$	expt
water/vacuum	53.4 (1.3)	56.3 (1.4)		4.1 (0.1)	70.0
heptane/vacuum	14.6 (2.4)	22.3 (3.0)		4.4 (0.1)	19.8
heptane/water	47.2 (2.8)	44.8 (2.8)	45.1 (4.0)	0.2 (0.1)	50.2
DPPC bilayer/water	18.2 (0.6)		18.3 (0.6)	0.8 (0.1)	

[a] Trajectory lengths are 11 ns for the bilayer and 600 ps for the others. The correction term $\Delta\gamma$ (evaluated from eq 5) should be added to values of γ calculated with $r_c = 10$ Å to take long-range LJ terms into account. Standard errors in parentheses.

water and heptane for $r_c = 10$ and 25 Å with experiment. In results similar to those obtained for bulk systems, the relative effects of simulating with a larger LJ cutoff are substantially larger for heptane than for water. This is because the water is relatively incompressible and the effects of electrostatic interactions (calculated with Ewald summation) dominate. For both systems adding $\Delta\gamma$ evaluated from eq 5 to the surface tensions obtained at $r_c = 10$ Å leads to results similar to those obtained with $r_c = 25$ Å, within statistical error.

Table 4 also compares heptane/water interfacial tensions calculated from simulations at NPAT and NPAT/LRC. The average value of ΔP_{zz} equaled 128.7 ± 0.6 atm. The difference between the two methods is smaller, because the vacuum space is replaced by another liquid, and the normal and tangential terms in $\Delta\gamma$ nearly cancel each other; i.e., $\Delta\gamma \approx 0$.

Turning to the DPPC bilayer,the average *D*-spacing (equal to L_z for the present system) evaluated from 1−11 ns intervals equaled 66.18 ± 0.01 and 65.50 ± 0.01 Å for simulations NPAT and NPAT/LRC, respectively, with $\langle \Delta P_{zz} \rangle = 196.1 \pm 0.1$ atm. As for the bulk systems, an increase in density (here manifested by a decrease in *D*-spacing) is an inevitable consequence of the LRC, and in this case it leads to worse agreement with the experimental value of 67 Å.[19] Interfacial tensions (Table 4) are not significantly altered by the application of the LRC, with $\Delta\gamma = 0.8 \pm 0.1$ dyn/cm. Because the LRC is independent of system size, $\Delta\gamma$ will also be independent; i.e., even though the magnitude of the membrane interfacial tension decreases as system size increases,[28] the LRC correction should be the same.

Summary and Conclusions

A straightforward method that accounts for the long-range LJ terms in constant pressure MD simulations has been developed. The LRC consists of an additional applied pressure, ΔP, which is calculated from the difference of instantaneous pressures at relatively short (r_c) and very long cutoffs (r_l) and updated as necessary. The values $r_c = 10$ Å and $r_l = 30$ Å are expected to be applicable to systems described with typical molecular mechanics force fields, and should be independent of system size. The update frequency of 10 ps used here can likely be increased after the system has reached equilibrium, or a heuristic method (such as described earlier) could be adopted. The method is particularly suited to anisotropic systems such as liquid/liquid interfaces and membranes, where ΔP is a tensor and the individual components can be applied separately. In general, the method may prove useful for any large heterogeneous macromolecular system where approximations based on a constant $g(r)$ are expected to fail. Because this LRC relies on adjustment of the pressure, corrections to the total energy of the system are not calculated (cf. eq 1). Hence, an additional long-range correction is still required when evaluating properties such as heats of vaporization, where the energies of liquid and gas phase systems are compared.

The feasibility of the method was demonstrated for a range of alkanes and bulk water. As might be anticipated, application of the LRC increases densities and decreases isothermal compressibilities for all systems studied (Table 1). Substantially improved agreement with experiment is obtained for the alkanes, although errors remain in the derived methyl and methylene volumes (Table 2). Translational diffusion constants and the NMR ^{13}C T_1 relaxation times are decreased for alkanes. However, agreement with experiment is generally poorer than for constant pressure simulations carried out with no correction (Table 3). This implies that the viscosities are too high even though the densities are correct. These results demonstrate the importance of including dynamic properties when parametrizing molecular mechanics force fields, and provide a starting point for future parametrization. The effects of the LRC are smaller for water (it is less compressible than the alkanes), and mixed: agreement for isothermal compressibility is improved, but is diminished for density. The latter result follows because the density of modified TIP3P water overestimates experiment when simulated at NPT.

The surface tension of the heptane/vacuum system was shown to be very sensitive to long-range LJ terms (Table 4), highlighting the need for the correction term $\Delta\gamma$ specified by eq 5. The relative contribution of long-range LJ terms to the surface tension of water (where electrostatic terms dominate) is smaller than for heptane, even though $\Delta\gamma$ is comparable. Simulations of heptane/water and a DPPC bilayer with and without the LRC yielded similar interfacial tensions, because corrections to the normal and tangential components in the pressure tend to cancel out in liquid/liquid interfaces. Nevertheless, other properties such as the density are sensitive to long-range LJ terms, and the LRC should be applied when simulating such interfaces.

Acknowledgment. This study utilized the high-performance computational capabilities of the Biowulf/LoBoS3 cluster at the National Institutes of Health, Bethesda, MD.

References and Notes

(1) Allen, M. P.; Tildesley, D. J. *Computer simulation of liquids*; Clarendon Press: Oxford, 1987.

(2) Steinbach, P. J.; Brooks, B. R. *J. Comput. Chem.* **1994**, *15*, 667.

(3) Darden, Y. D.; York, D.; Pedersen, L. *J. Chem. Phys.* **1993**, *98*, 10089.

(4) Smith, P. E.; van Gunsteren, W. F. Methods for the Evaluation of Long-Range Electrostatic Forces in Computer Simulations of Molecular Systems. In *Computer Simulation of Biomolecular Systems: Theoretical and Experimental Applications*; van Gunsteren, W. F., Weiner, P. K., Wilkinson, A., Eds.; ESCOM: Leiden, 1993; Vol. 2, pp 182−212.

(5) Feller, S. E.; Pastor, R. W.; Rojnuckarin, A.; Bogusz, S.; Brooks, B. R. *J. Phys. Chem.* **1996**, *100*, 17011.

(6) Essmann, U.; Perera, L.; Berkowitz, M. L.; Darden, T.; Lee, H.; Pedersen, L. G. *J. Chem. Phys.* **1995**, *103*, 8577.

(7) Alper, H. E.; Bassolino, D.; Stouch, T. R. *J. Chem. Phys.* **1993**, *98*, 9798.

(8) Alper, H. E.; Bassolino, D.; Stouch, T. R. *J. Chem. Phys.* **1993**, *99*, 5547.

(9) MacKerell, A. D.; Bashford, D.; Bellott, M.; Dunbrack, R. L.; Evanseck, J. D.; Field, M. J.; Fischer, S.; Gao, J.; Guo, H.; Ha, S.; Joseph-McCarthy, D.; Kuchnir, L.; Kuczera, K.; Lau, F. T. K.; Mattos, C,; Michnick, S.; Ngo, T.; Nguyen, D. T.; Prodhom, B.; Reiher, W. E.; Roux, B.; Schlenkrich, M.; Smith, J. C.; Stote, R.; Straub, J.; Watanabe, M.; Wiorkiewicz-Kuczera, J.; Yin, D.; Karplus, M. *J. Phys. Chem. B* **1998**, *102*, 3586.

(10) Brooks, B. R.; Bruccoleri, R. E.; Olafson, B. D.; States, D. J.; Swaminathan, S.; Karplus, M. *J. Comput. Chem.* **1983**, *4*, 187.

(11) Feller, S. E.; MacKerell, A. D., Jr. *J. Phys. Chem.* **2000**, *104*, 7510.

(12) Jorgensen, W. L.; Chandrasekhar, J.; Madura, J. D.; Impey, R. W.; Klein, M. L. *J. Chem. Phys.* **1983**, *79*, 926.

(13) Durell, S. R.; Brooks, B. R.; Ben-Naim, A. *J. Phys. Chem.* **1994**, *98*, 2198.
(14) Ryckaert, W. E.; Ciccotti, G.; Berendsen, H. J. C. *J. Comput. Chem.* **1977**, *23*, 327.
(15) Feller, S. E. Personal communication.
(16) Woolf, T. B.; Roux, B. *Proteins: Struct., Funct., Genet.* **1996**, *24*, 92.
(17) Bernèche, S.; Nina, M.; Roux, B. *Biophys. J.* **1998**, *75*, 1603.
(18) Allen, T. W.; Andersen, O. S.; Roux, B. *J. Am. Chem. Soc.* **2003**, *125*, 9868.
(19) Nagle, J. F.; Tristram-Nagle, S. *Biochim. Biophys. Acta* **2000**, *1469*, 159.
(20) Small, D. M. *The Physical Chemistry of Lipids*; Plenum Press: New York, 1986.
(21) Press, W. H.; Teukolsky, S. A.; Vettering, W. T.; Flannery, B. P. *Numerical Recipies*; Cambridge University Press: New York, 1992.
(22) Holz, M.; Heil, S. R.; Sacco, A. *Phys. Chem. Chem. Phys.* **2000**, *2*, 4740.
(23) Douglass, D. C.; McCall, D. W. *J. Phys. Chem.* **1958**, *62*, 1102.
(24) Lipari, G.; Szabo, A. *Biophys. J.* **1980**, *30*, 489.
(25) Ottiger, M.; Bax, A. *J. Am. Chem. Soc.* **1998**, *120*, 12334.
(26) Lyerla, J. R.; McIntyre, H. M.; Torchia, D. A. *Macromolecules* **1974**, *7*, 11.
(27) Zhang, Y.; Feller, S. E.; Brooks, B. R.; Pastor, R. W. *J. Chem. Phys.* **1995**, *103*, 10252.
(28) Feller, S. E.; Pastor, R. W. *Biophys. J.* **1996**, *71*, 1350.